Proceedings, 11th FIG Symposium on Deformation Measurements, Santorini, Greece, 2003.

MONITORING VERTICAL MOVEMENTS IN MOUNT CARMEL REGION

Gilad Even-Tzur

Department of Civil and Environmental Engineering,
Technion – Israel Institute of Technology, Haifa 32000, Israel

Abstract

The Mount Carmel fault is one of the major geological structures in northern Israel. The fault is characterized by intense and continuous seismic activity, which marks the Carmel region as potentially hazardous.
In order to monitor movements in the Carmel region a small network, spanning an area of 40 by 30 km. and consisting of 17 points, was constructed. Four sets of GPS measurements were taken between 1990 and 1999. For additional improvement of the monitoring ability of vertical movements two campaigns of precise leveling were carried in the monitoring region.
Two-Step analysis of the GPS measurements in the Carmel monitoring area was carried out to quantify recent vertical tectonic deformations. In this study the precision leveling data from the Survey of Israel is used in addition to the GPS measurements for quantifying vertical deformations in order to improve our understanding of the vertical movements in the Carmel region.
Strict analysis of the GPS and the leveling data shows significant vertical movements in the area. Two independent methods are pointing to the same vertical behavior at the monitored region. The Carmel range uplifts at a rate of 5 mm/yr relative to its surroundings.

1. Geological background

The geology of Israel is dominated by the Dead Sea rift, which separates the Arabian plate from the African plate. It runs from the Red Sea in the south through the Dead Sea, and north along the Jordan River, the Lake of Galilee and up through the Baqqa Valley in Lebanon towards the Taurus mountains in Turkey. Its influence on the geological structure in northern Israel is strongly pronounced in secondary faulting, which run in a general northwesterly direction. One such secondary fault is the Carmel-Tirza fault system. The Carmel-Tirza fault zone is composed of several NW-SE trending small faults, including the Tirza fault, the Gilboa fault and the Carmel fault in the north, which extends into the Mediterranean Sea (Ben-Gay and Ben-Avraham, 1995).
The Carmel fault is one of the major geological structures in the northern part of Israel. It borders Mount Carmel from the north and the west (see fig. 1). The fault is characterized by intense and continuous seismic activity (Hofstetter et al., 1996). The fault area is known to be of complex geological and tectonic structure (Achmon, 1986; Ron et al., 1991), with an inland structural uplift of more than 500 meters above sea level.
The Carmel fault is a strike-slip fault. The lateral offset across is more then 3-4 km over the last 20 million years (Achmon, 1986). The Carmel fault is divided into three distinct segments (Rotstein et al., 1993), which can bee seen in fig. 1. In its southern part the fault trends NW-SE, and is characterized by simple a strike-slip motion, and its deformation is limited to a distinct fault zone. East of Mount Carmel the fault assumes a N-S trend with intense deformation in a zone several kilometers wide. Further to the northwest, the fault resumes its NW-SE trend with decreased deformation.

In the middle segment a component of E-W compression exists as result of the strike-slip environment. The compression is associated with active uplifting (Rotstein et al., 1993).

2. The GPS Measurements Campaigns

The GPS network was basically planned to monitor horizontal movements. In planning the network we were guided by the assumption of three relatively rigid blocks in the area (see fig. 1), which are in a state of lateral motion with respect to each other. Each block was marked by at least four points. The block east of the fault (lower Galilee and Tivon-Hills) was marked by seven points because of its extent and apparent inhomogeneity. The northern Carmel block was marked by six points due to its designation to serve in defining the Carmel network datum. The designing was concluded with 17 points for the whole monitoring network.
The network points were marked, without an exception, on exposed and solid bedrock by 15-centimeter long iron nails, which were concreted into drilling holes in the bedrock.

The first GPS campaign was carried out during one week in September 1990. It has been the first GPS monitoring operation that was carried out in Israel for the purposes of geodynamic research. The network was measured by three single frequency model L-XII Ashtech receivers. 13 GPS satellites allowed for a measurement window of 10 hours a day, with 3-4 satellites above the horizon. The measurement time of a session ranged between 75 to 90 minutes. In total 23 sessions were measured, about four sessions per day.
Analysis of the accumulated data in 1990 revealed serious weaknesses in the network and caused an extension of the data collection stage into 1991 (Papo and Even-Tzur, 1992). Data from point #7 in the east turned to be insufficient in quantity. Due to limited resources it was decided to avoid measuring point #7 again in this campaign.
The second campaign was carried out in April 1991. Following a mistaken analysis of the first campaign the session configuration design was improved. Emphasis was put on antenna height measurement, and the session time was increased to 120 minutes at least. The GPS satellite constellation included 15 satellites providing coverage of 24 hours with a minimum of three satellites. 19 sessions were measured by three L-XII Ashtech receivers. All the network points were measured, besides point #1 in the north, which was destroyed in the beginning of 1991.
The third campaign was carried out in 1994. This campaign was not measured for geodynamic purposes, but as part of the undulation project that was measured by the Survey of Israel. Only 10 points from the Carmel monitoring network were measured as part of a network that contained more than 60 points. The quality demands from the network measured in the undulation project were not high as expected from monitoring deformation networks, which could lead to low quality results. The data from the 1994 campaign was included for four main reasons: dual frequencies receivers measured the network (Trimbel 4000SSE), the number of the GPS satellites had increased dramatically since 1991, the degrees of freedom in the undulation project were high, and the fact that till 1999 no other monitoring campaign was carried in the Carmel network.
The fourth campaign was measured in December 1999. All the lessons from former campaigns were implemented. Each session was measured for at least three hours. In each point the antenna was set up twice, independently, to increase the ability of gross error detection. The network was measured by six dual frequencies Ashtech receivers (three M-XII, two Z-surveyors, and one Z-12). The Carmel network was extended by five points from the Geodetic-Geodynamic network of Israel and one permanent GPS station (BSHM), located at the Technion campus near point #10 (see fig. 1). In this manner two points were added to the northern Carmel, two point to the southern Carmel and two points to the lower Galilee. Four points from the original network were destroyed during the years (point number #1, #3, #6, and #8) due to massive development in the region.
In all campaigns geodetic antennas were used.
The longest measured vector in the Carmel network is of 26 km and the average length is of 10 km.

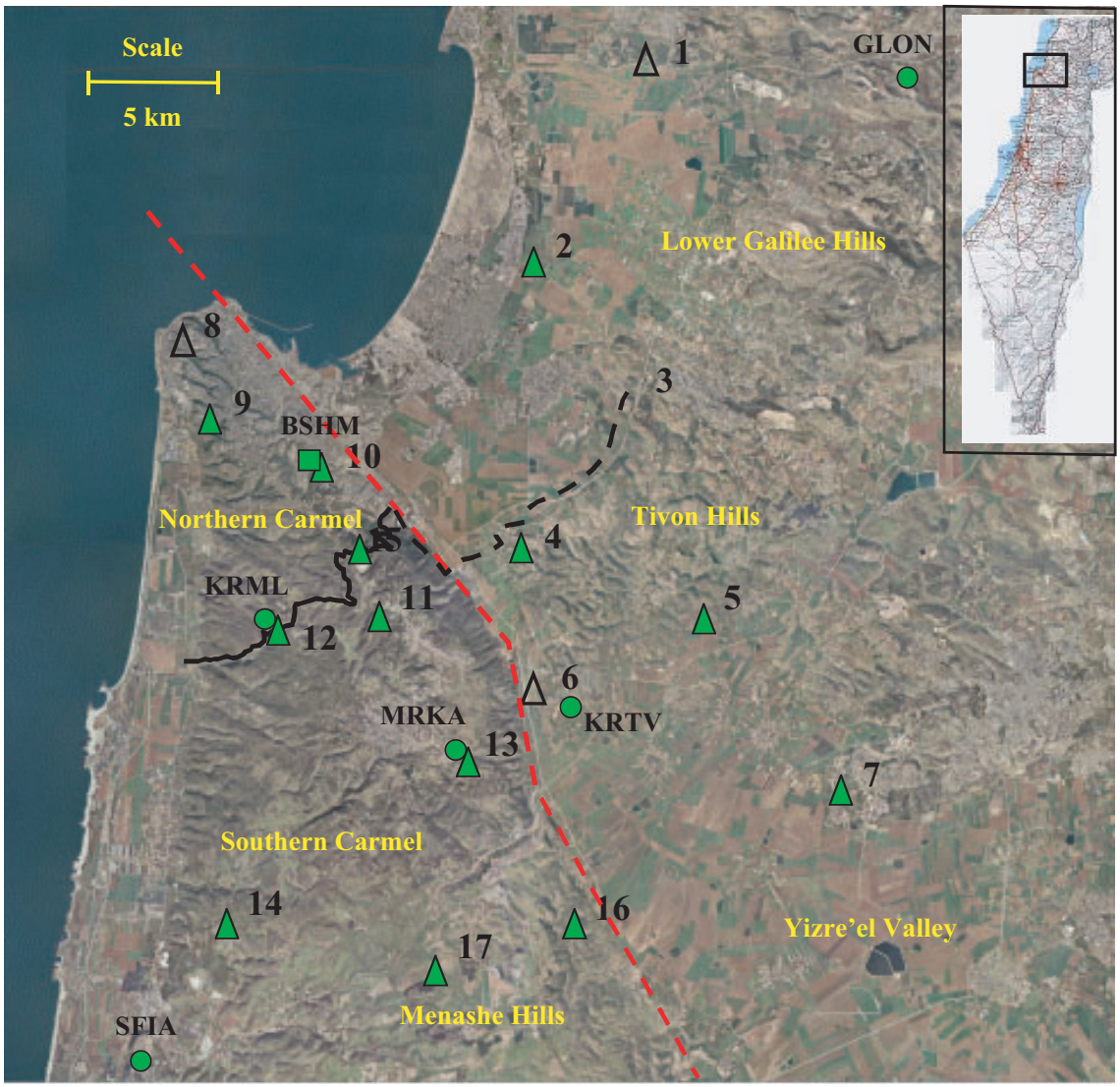

Figure 1 - Image of the Carmel region. Green solid triangle – Point of the Carmel deformation-monitoring network. Green triangle – Destroyed points. Green circle – Point of the Geodetic-Geodynamic network in Israel. Green square – Permanent GPS station.Solid black line – The leveling line. Broken black line – The extension of the leveling line.
Broken red line - The Carmel fault.

3. Analysis of GPS Phase Observation

The GPS data from all the campaigns were collected over almost ten years, and was analyzed with the AOS (Ashtech Office Suite), which is a single baseline processor software. The 1990 and 1991 campaigns were processed shortly after they were measured by the Ashtech software GPPS (GPS Post Processing Software). At the beginning of 2000 samples of several sessions were processed by AOS to compare the results. Significant differences were found in the vector components, but the vector length remained the same, therefore it was decided to process all the campaigns with the same software.

All sessions were processed using precise ephemeris. In the IGS web site precise ephemeris can be find since the year 1994. Thanks to Mr. Don Haw from the National Geodetic Survey we were able to get the precise ephemeris for the 1990 and 1991 campaigns.

Some problems were encountered while converting the old GPS Ashtech data format to the current format available for the AOS. Despite ample assistance from Ashtech, a complete conversion of all the data was not achieved, therefore the number of processed vectors

decreased relative to the number of measured vectors. Table 1 summarizes the GPS field surveying and observation process.

Table 1 - Summary of GPS field surveying and observation process

Year	**1990**	**1991**	**1994**	**1999**
Receiver Type	L1 wave C/A-code	L1 wave C/A-code	L1/L2 waves C/A+P-codes	L1/L2 waves C/A+P-codes
Epoch interval [s]	20	20	15	30
Satellites above horizon	3-4	3-4	5+	5+
Average of Session duration [h:mm]	1:30	2:00	1:00	3:00
Number of receivers	3	3	2-6	6
Number of Sessions	23	19	17	6
Number of measured vectors	67	57	98	94
Number of processed vectors	48	43	95	94
Number of measured points	17	16	30	19

4. Network Adjustment and Deformation Analysis

The algorithm implemented to detect vertical movement is a series of campaigns analysis by the Two-Step analysis method (Agmon, 2001; Papo and Perelmuter, 1993), using a kinematical model of velocities as the model of motion (Papo and Perelmuter, 1984). The analysis is based on the partitioning of the surveyed area into sub-areas based on geological criteria. According to these criteria each sub-area is characterized as a geological block, in which motion is homogenous. The algorithm is based on describing the relative motion between the blocks and the internal motion within each block. The Two-Step method divides the observations adjustment made to a motion model into two steps. The first step is a rigid adjustment of each single campaign to a network of points. In the second step a model is suggested and tested to best fit the changes in the point positions over time. The single network serves as pseudo-observations to the second step adjustment. The residuals of the second step adjustment are known as the model noise. Generally, smaller residuals indicate a better fitness for use of the suggested model.

The first step of analysis shows good network in 1999 and 1994 and weaknesses in 1990 and 1991. The quality of the two initial campaigns was not good enough to consider them as monitoring epochs. Single frequency receivers, small number of satellites in view, and short sessions caused the low quality of the network. In an attempt to increase the initial network quality it was decided to combine the two monitoring epochs, from 1990 and 1991, and consider them as one epoch. The fact that no significant movement was detected between the two monitoring epochs (Even-Tzur, 1991), and the short time lapse between them (only 7 months) justifies the unity.

The quality of the network obtained in the 1994 campaign may seen misleadingly good but it may be wrong impression. The vectors quality was good, as they were short in length and measured by high quality receivers. But the measurement sessions were of short duration, and not many vectors were connected to each network point. It was decided to use the 1994 epoch since it enable a series of monitoring epochs and will therefore support the acceptance or rejection of the vertical motion model. Table 2 summarizes the network adjustment for each monitoring epoch.

Table 2 - Free network adjustment- summary of each monitoring epoch.

Year	**1990+91**	**1994**	**1999**
Number of Adjusted Vectors	75	90	90
Number of Adjusted Points	17	30	19
Number of Common Points with the 1990+91 Campaign	17	10	13
Degrees of Freedom	177	183	216
Variance of Unit Weight, $\hat{m}_0^2$	1.005	1.082	0.990
Average σ of Vertical Measured Component [mm]	24	22	22
One σ of Vertical Adjusted Point [mm]:			
Average	8.9	10.3	7.1
Minimum	5.8	5.9	3.5
Maximum	18.5	18.3	14.1

Each monitoring epoch was solved with minimum constraints. The same constraints were used in all epochs for achieving the minimum constraints solution. The results of this first step were sets of the network point coordinates, pertaining to the specific epochs of the measurements. The minimum constraints solution, their relative cofactor matrix, the variance of unit weight, and the degree of freedom from each monitoring epoch were used as pseudo-measurements in the second step.

The accuracy estimation of a processed vector by AOS is over optimistic and does not reflect the actual accuracy of the measured vector. We therefore multiplied the variance-covariance matrix processed by the software by a specific factor for obtaining more realistic accuracy estimation. The factor used for the three monitoring epochs was 12.

For k receivers there are $k(k-1)/2$ single vectors, while only k-1 of these vectors are independent. To compensate for the artificial increase of redundancy, as a result of using all possible vectors, the normal matrix was multiplied by factor $2/k$ (Han and Rizos, 1995).

The minimum constraints solutions and their respective corrected variance-covariance matrices were transformed into free networks. The trace of the variance-covariance matrix was minimized and reflected only the relative accuracy of the point positions (see table 2), without the influence of the reference system choice, thus enabling the evaluation of the quality of the GPS campaigns.

The adjusted heights of the network points in local horizontal system relative to point #10 and their accuracies can be seen in table 3.

The residuals **v** and their cofactor matrix $\mathbf{Q}_v$ were used as a basis for gross errors deduction in a significant level of 5%, using the appropriate statistical test (Chen et. al, 1987), while the three components of each vector were tested simultaneously.

In the second step a kinematical model of vertical velocities was used as the model of motion. The suggested model was tested to best fit the changes in the vertical point positions over time.

The vectors of vertical heights $\mathbf{x}_i$ at a given moment t_i are used to estimate the coordinates of the network points $\mathbf{x}_0$, for a reference epoch t_0 and the velocity of the points $\dot{\mathbf{x}}$, by using the kinematical model:

$$\mathbf{x}_i = \mathbf{x}_0 + \dot{\mathbf{x}}\,(t_i - t_0) \tag{1}$$

Where in this case i=1,2,3 as the three monitoring epoch campaigns that were measured.

The observation equation system for three epochs of measurements is the following:

$$\begin{bmatrix} \mathbf{x}_1 \\ \mathbf{x}_2 \\ \mathbf{x}_3 \end{bmatrix} = \mathbf{B}\begin{bmatrix} \mathbf{x}_0 \\ \dot{\mathbf{x}} \end{bmatrix} + \mathbf{w} \tag{2}$$

where **B** denotes the Jacobian matrix, and is usually a full column rank matrix, and **w** is the model noise vector. Generally, smaller residuals indicate a better fitness for use of the suggested

model. $\mathbf{x}_0$ and $\dot{\mathbf{x}}$ are solved based on the minimum constraint solutions $\mathbf{x}_i$, then transferred into a free solution, which is used to determine vertical movements.

The velocity vector $\dot{\mathbf{x}}$ and its cofactor matrix $\mathbf{Q}_x$ can be transformed into a common datum definition by the following similarity transformation:

$$\hat{\mathbf{x}}_1 = \mathbf{J}\hat{\mathbf{x}} \qquad \hat{\mathbf{x}}_1 = \mathbf{J}\hat{\mathbf{x}} \tag{3}$$
$$Q_{\hat{x}_1} = J Q_{\hat{x}} J^T$$
$$J = I - G(G^T P_x G)\, G^T P_x$$

Where $\mathbf{x}_1$ and its cofactor matrix $\mathbf{Q}_{\dot{x}}$ are the velocity vector and its cofactor matrix, based on the new datum, **J** is the similarity transformation matrix constructed on the basis of the union of the datum defect in the monitoring epochs and on the number of common points. $\mathbf{P}_x$ is the weight matrix, where 1 stands for points that enter the datum definition and 0 stands for all other points (Papo and Perelmuter, 1984). When $\mathbf{P}_x$ equals the identity matrix ($\mathbf{P}_x = \mathbf{I}$), all points in the network are defined as a datum, and we achieve minimum trace solution. Using **J** we can easily transform the solution and its cofactor matrix from one reference point system to another.

Table 3 - The adjusted heights ($\mathbf{x}_i$) of the monitoring network points relative to point #10 in local horizontal system (all units are in meter) for three monitoring epochs.

Point #	1990+91		1994		1999	
	Up	σ_{Up}	Up	σ_{Up}	Up	σ_{Up}
01	-203.9802	0.0149	-		-	
02	-188.8745	0.0112	-188.8737	0.0078	-188.8955	0.0079
03	-137.1158	0.0093	-137.1224	0.0097	-	
04	-156.8795	0.0089	-156.8942	0.0116	-156.9100	0.0081
05	-66.4646	0.0114	-66.4709	0.0165	-66.5040	0.0088
06	-158.5348	0.0111	-		-	
07	-89.5145	0.0214	-		-89.4805	0.0110
08	-64.5747	0.0131	-		-	
09	-66.3255	0.0085	-		-66.3167	0.0072
10	0.0000	0.0000	0.0000	0.0000	0.0000	0.0000
11	331.4696	0.0078	331.4627	0.0133	331.4900	0.0063
12	44.9734	0.0090	44.9622	0.0158	44.9466	0.0058
13	244.5009	0.0111	244.4224	0.0180	244.5094	0.0069
14	-165.5484	0.0135	-165.6356	0.0216	-165.5998	0.0089
15	159.4839	0.0069	159.4968	0.0177	159.5014	0.0054
16	-84.2931	0.0131	-		-84.2805	0.0119
17	-6.5347	0.0132	-6.5917	0.0198	-6.5264	0.0084

Based on prior geological information a group of points was set as datum and tested for its stability by using congruency testing (Setan and Singh, 2001). Unlike the northern Carmel, the southern Carmel is rich with small geological faults, running from the west to the east. There is no indication that one of them is active (Achmon, 1986). Despite this, the small amount of geological faults in the northern Carmel increases its potential for serving as a datum.

The northern Carmel points (#9, #10, #11, #12, #15) were set as datum. In a significance level of 5% the points were proven to be unstable. Omitting point #12 from the datum lead to stability, which means that the northern Carmel does not behave homogenously in the vertical dimension. Adding point #13 to the datum definition was accepted despite of its pertinence to the southern Carmel region. Looking at the Carmel map (fig. 1) one can see that the datum points cover the central range line of mount Carmel from north to south.

Relative to the datum definition the velocity of the lower Galilee and Tivon-Hills points is 5 mm/yr in the negative direction (see table 4). The velocities of points #3 and #7 are not significant. The velocity of point #3 is in the range of near by points but its accuracy is low. The point was measured twice and destroyed after the 1994 campaign.

The velocities of the points located on the western hillside of mount Carmel increase, when moving away from the central range line, in up to 6 mm/yr for point #14.

The velocities of points #16 and #17, located on Menash-Hills, are not significant.
The results demonstrate a vertical uplift of the mount Carmel range relative to the surrounding area. The Carmel range uplifts significantly relatively to the Tivon-Hills from the east and to the coastline from the west, in the rate of about 5 mm/yr.

Table 4 - The vertical velocities of the Carmel network points relative to the Mount Carmel central range line.

Point #	$\dot{x}$ [mm/yr]	$2\sigma_{\dot{x}}$ [mm/yr]
Datum Points		
09	-0.37	2.07
10	-1.43	1.58
11	0.80	1.48
13	0.49	2.22
15	0.51	1.38
Object points		
02	-5.73	4.50
03	-4.15	7.56
04	-5.05	2.54
05	-5.40	3.08
07	2.45	5.76
12	-4.38	1.98
14	-6.65	3.44
16	-0.14	3.93
17	-0.86	3.31

5. The Leveling Measurements Campaigns

Precise leveling data from the Survey of Israel (SOI) was used to improve the understanding of the recent vertical movements in the Carmel region.
The relevant leveling data is from a leveling line that starts at the coastline in the west side of the Carmel mountain near Atlit (BM 719A), and across the mountain till Nesher (BM 1165), which is located at the east side of the Carmel mountain (see fig. 1 and 2). The total line length is 20 km and it contains 31 benchmarks. The line was leveled twice between May 1987 and December 1992 with four sections that were leveled more than twice. All sections were independently double leveled and measured with precise values in accordance with the rules of the International Association of Geodesy.

6. Analysis of the leveling data

The vertical velocities were calculated using the differences in height between sequential benchmarks, which were measured using a process of front to back and vise versa measurements, and the time laps between sequential leveling campaigns. The leveling data was taken from the original books kept in the SOI archive.

The standard deviation in millimeters (σ) of the differences in height between every two benchmarks was obtained from difference of two measures. In total there were 71 pairs of measurements. Because of the mountainous characteristics of the region, the number of level set-up (SU) is used as the basis for weight assigning. The standard deviation of height differences, based on a single level set up is $\sigma_0 = 0.1$ mm. In average the number of level set up per one kilometer is 40 thus the standard deviation of the differences in height between two benchmarks for a distance of one kilometer is 0.67 mm. If the time interval between two epochs of observation is Δt , then the standard deviation of the velocity between two benchmarks is:

$$\sigma_{\dot{x}} = \sqrt{\frac{\sigma_0^2}{\Delta t^2}\,(\text{number of SU})} \qquad (4)$$

When more than two differences of height between two benchmarks were measured, the velocity and its standard deviation were computed by means of adjustment computation.

As in the analysis of the Carmel GPS monitoring network by similarity transformation the benchmarks located in the central range were set as datum. Nine benchmarks numbered 4883 to 4887 can be used as datum points with a significance level of 5%. When shifting away from the central range the velocity increases by 5 mm/yr in the west side and 2 mm/yr in the east side, where the velocities are significant.

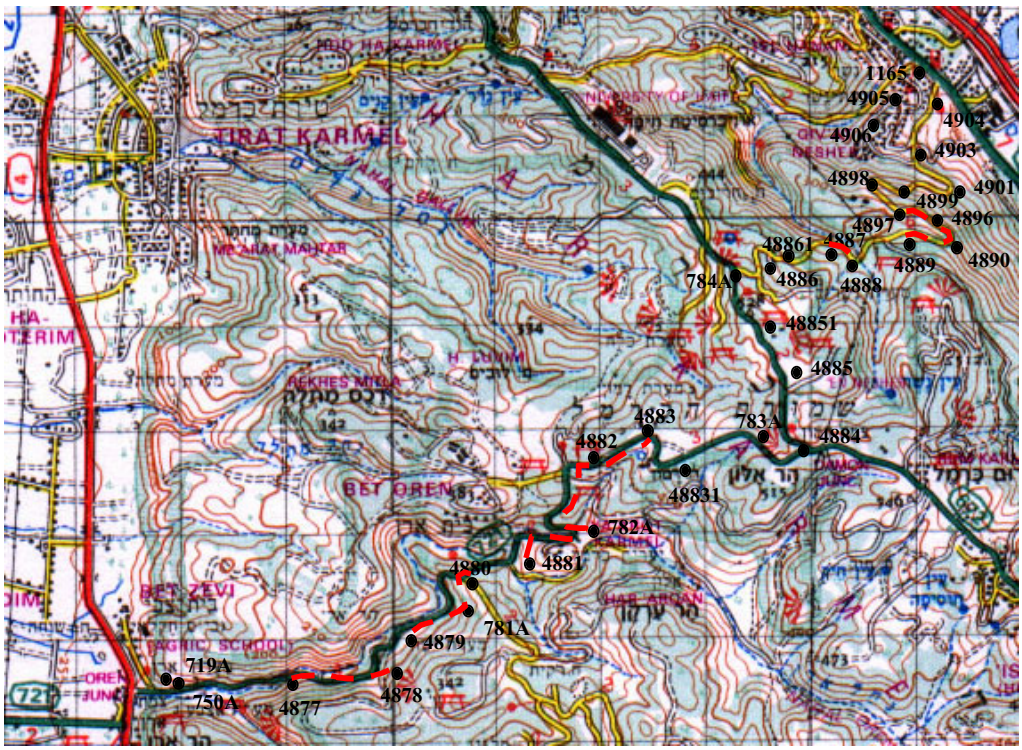

Figure 2 - The location of the benchmarks along the leveling line from Atlit (719A) to Nesher (1165). Read broken line stands for leveling sections with significant velocity with respect to the previous benchmark.

Table 5 - The vertical velocities of the benchmark relative to the datum points.

BM	$\dot{x}$ [mm/year]	$2\sigma_{\dot{x}}$ [mm/year]	
719A	-5.763	1.363	**Object points**
4877	-5.556	1.309	
4878	-4.764	1.226	
4879	-4.744	1.195	
781A	-4.268	1.141	
4880	-3.901	1.104	
4881	-3.553	1.027	
782A	-2.746	0.942	
4882	-1.554	0.635	
4883	-0.433	0.545	**Datum Points**
48831	-0.185	0.440	
783A	-0.074	0.353	
4884	-0.037	0.328	
4885	0.116	0.317	
784A	0.226	0.368	
4886	0.329	0.402	
48861	0.172	0.441	
4887	-0.115	0.526	
4888	-0.446	0.571	**Object points**
4889	-0.676	0.666	
4890	-0.920	0.709	
4896	-1.396	0.755	
4897	-0.760	0.781	
4898	-0.760	0.812	
4899	-1.022	0.856	
4900	-1.166	0.880	
4901	-1.303	0.921	
4902	-1.421	0.942	
4903	-1.236	0.962	
4904	-1.443	1.018	
1165	-1.635	1.045	

To The West

Carmel Range

To The East

7. Summary and Discussion

In order to monitor movements in the Carmel region a small network, spanning an area of 40 by 30 km. and consisting of 17 points, was constructed. Four sets of GPS measurements were carried out over a period of nine years. In this study precise leveling data from SOI is used along with GPS data to quantify vertical deformation in an attempt to improve the understanding of the Carmel area vertical movements.

The analysis of the Carmel monitoring network epochs using the Two-Step analysis revealed significant results. Strict analysis of the GPS and leveling data showed significant vertical movements on Mount Carmel. The Carmel range uplifts in a rate of 5 mm/yr relative to its surrounding. However, this uplift must be examined carefully, as the movements of the Carmel may be viewed as uplift or as sinking of the surroundings, depending upon the point of reference. It is important to note that differential GPS and leveling measurements cannot define an absolute reference frame.

Two independent methods used have pointed out to the same vertical behavior at the monitored region.

The same geographic area was used as datum for the GPS network and for the leveling line. We can conclude that the central range area of the Carmel Mountain is vertically stable.

The Carmel network point #12 is located very near to benchmark 4880 and point #15 is located near benchmark 4887. The velocity of point #15 relative to point #12 is 4.9±1.1 mm/yr. The

velocity of benchmark 4887 relative to benchmark 4880 is $3.8 \pm 0.7 \text{mm/yr}$. This may serve to further demonstrate our claim, as the velocities are statistically similar. This example sharpens the similar resemble the results we get from the GPS and the leveling data about the vertical behavior of points in the monitored region.

Additional monitoring campaigns should be measured in the Carmel region for the purpose of observing future vertical movements in the area. Additional data will enable more precise testing of the suitability of the kinematical model in the region. It will also enable testing other deformation models besides the kinematical model.

In the coming weeks the leveling line will be measured again, from Atlit in the west side of the Carmel Mountain to Nesher in the east. This time the leveling line will extend from Nesher to the Tivon-Hills up to the Lower Galilee Hills (see fig. 1). The extended part of the leveling line was measured for the first time in 1986. This extension will allow an examination of the behavior of the east side slope of the Carmel Mountain relative to the Tivon-Hills, and enable comparesing it to the results of the Carmel network.

References

Achmon, M. (1986). *The Carmel Border Fault*. M.Sc. Thesis, The Hebrew University, Jerusalem, Israel (in Hebrew).

Agmon, E. (2001). *Algorithm for the Analysis of Deformation Monitoring Networks*. M.Sc. Thesis, Technion, Israel Institute of Technology, Israel (in Hebrew).

Ben-Gai, Y. and Z. Ben-Avraham (1995). Tectonic Processes in Offshore Northern Israel and the Evolution of the Carmel Structure. *Marin and Petroleum Geology*, 12(5), 533-548.

Chen, Y.Q., M. Kavouuras, A. Chrzamowski (1987). A Strategy for Detection of Outlying Observations in Measurements of High Precision. *The Canadian Surveyor*, 41(4), 529-540.

Even-Tzur, G. (1991). *Monitoring Deformation in the Carmel Mountain Region by GPS*. M.Sc. Thesis, Technion, Israel Institute of Technology, Israel (in Hebrew).

Han, S., and C. Rizos (1995). Selection and Scaling of Simultaneous Baselines for GPS Network Adjustment. *Geomatics Research Australasia*, 63, 51-66.

Hofstetter, A., T. van Eak, A. Shapira (1996). Seismic Activity Along Fault Branches of the Dead Sea-Jordan Transform System: The Carmel-Tirza Fsult System. *Tectonophysics*, 267, 317-330.

Papo, H.B., and G. Even-Tzur (1992). Monitoring Deformation in the Carmel Mountain Region by GPS Measurements. *Sixth International Geodetic Symposium on Satellite Positioning, Ohio, USA*.

Papo, H.B., and A. Perelmuter (1993). Two-Step Analysis of Dynamical Networks. *Manuscripta Geodetica*, 18(6), 422-430.

Papo, H.B., and A. Perelmuter (1984). Pre–Zero-Epoch Covariance Matrix in Sequential Analysis of Deformations. *Bulletin Geodesique*, 58, 75-83.

Ron, H., A. Nur and A. Hofstetter (1991). Late Cenozoic and Recent Strike Slip Tectonics in Mt. Carmel, Northern Israel. *Annales Tectonicae*, 4(2), 70-80.

Rotstein, Y., I. Bruner, U. Kafri (1993). High Resolution Seismic Imaging of the Carmel Fault and its Implications for the Structure of Mt. Carmel. *Israel Journal of Earth Science*, 42, 55-69.

Setan, H., and R. Singh (2001). Deformation Analysis of a Geodetic Monitoring Network. *Geomatica*, 55(3), 333-346.